

SCIENTIFIC REPORTS

There are amendments to this paper

OPEN

Activation of liver stromal cells is associated with male-biased liver tumor initiation in *xmrk* and *Myc* transgenic zebrafish

Qiqi Yang¹, Chuan Yan ^{1,2} & Zhiyuan Gong^{1,2}

Hepatocellular carcinoma (HCC) is more prevalent in men than in women. Previously we have found that some stromal cells, including hepatic stellate cells (HSCs), neutrophils and macrophages, play crucial roles in promoting sex disparity in *kras*^{V12}-induced zebrafish HCC. The activation of HSCs is mediated by serotonin while activation of neutrophils and macrophages is mediated by cortisol. To ensure that these findings are also applicable to other oncogene induced tumors, stromal cell activation was compared between male and female fish during liver tumorigenesis initiated by *xmrk* or *Myc* oncogene. Consistently, we observed male-biased liver tumorigenesis in the *xmrk* and *Myc* models. In both models, there was a higher rate of HSC activation accompanied with a higher level of serotonin in male liver tumors. For tumor-infiltrated neutrophils and macrophages, significantly higher densities in male liver tumors were observed in both *xmrk* and *Myc* models. However, the male-biased increase of cortisol was observed only in *xmrk*- but not apparently in *Myc* expressing liver tumors. Overall, these observations are consistent with the observations in the *kras* liver tumor model, indicating that the serotonin- and cortisol-mediated pathways also play roles in sex disparity of liver tumors caused by other molecular pathways.

Hepatocellular carcinoma occurs more frequently and aggressively in men than in women¹. Based on the animal model studies, the gender disparity might be owing to a sex hormone related mechanism, with a stimulating role of androgen and an inhibitory role of estrogen². Administration of estrogens inhibits HCC development in diethylnitrosamine (DEN)-treated male mice. On the contrary, ovariectomy or testosterone supplement increase occurrence of HCC in female mice³. However, clinical trials targeting sex hormone pathways, e.g. by using the estrogen receptor modulator tamoxifen, synthetic progestin (megestrol) and androgen antagonist flutamide, produced inconclusive results as these treatments in the clinical trials did not show significant improvement⁴⁻⁷.

Most of HCC arise on a background of hepatic fibrosis and/or inflammation and it has been increasingly recognized that some stromal cells in the tumor microenvironment (TME) are abnormally activated in both HCC animal models and HCC patients. Hepatic stellate cells (HSCs) are the main matrix-producing cells in the TME and play key roles in the progression of liver fibrosis. Co-culture of HSCs with HCC cells showed upregulated expression of proinflammatory cytokines and proangiogenic genes⁸. Depletion of HSCs from pre-established fibrosis attenuated fibrogenesis in a mouse liver disease model⁹. Co-transplantation of human intratumoral HSCs with HCC into nude mice showed enhanced HCC progression by HSCs and HSC density is correlated with the overall and recurrence-free survival, thus providing promising prognostic biomarkers¹⁰. Consistent with this, we also reported recently that HSC has a higher density and activation ratio in *kras*^{V12}-expressing tumor in the zebrafish¹¹.

Tumor associated macrophages (TAMs) and tumor associated neutrophils (TANs) play key roles in hepatic inflammation and cytokines produced by TAMs promote tumor growth, angiogenesis and suppression of adaptive immunity¹². DEN administration promotes IL-6 production in Kupffer cells in male mice and ablation of IL-6 attenuates liver carcinogenesis in male and abolishes the gender difference¹³. In HCC patients after resection, the

¹Department of Biological Sciences, National University of Singapore, Singapore, Singapore. ²National University of Singapore graduate school for integrative sciences and engineering, National University of Singapore, Singapore, Singapore. Qiqi Yang and Chuan Yan contributed equally to this work. Correspondence and requests for materials should be addressed to Z.G. (email: dbsgzy@nus.edu.sg)

Received: 31 May 2017

Accepted: 9 August 2017

Published online: 04 September 2017

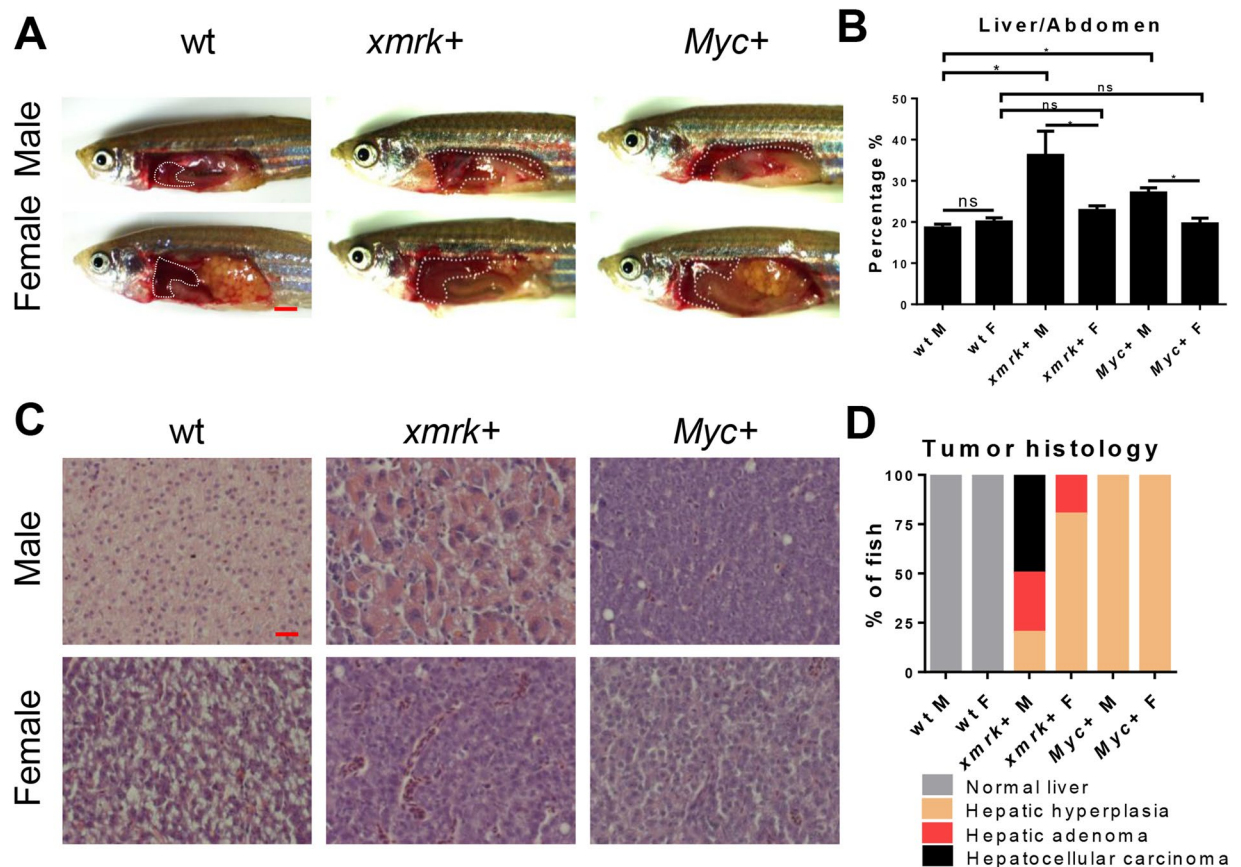


Figure 1. Characterization of sex disparity in *xmrk* and *Myc*-induced HCC progression. Three-month-old, *xmrk*⁺, *Myc*⁺ and wildtype zebrafish were treated with 60 μg/ml dox for 7 days. 10 fish were analysed in each group and the experiment was repeated multiple times. **(A)** Gross morphology of male and female fish (left lateral view). The livers are outlined. **(B)** Quantification of percentage of liver area to abdomen area. **(C)** Representative images of liver sections of male and female fish after H&E staining. **(D)** Quantification of tumor histology in male and female fish. *P < 0.05. Scale bars: 2 mm in **(A)** and 20 μm in **(C)**.

number of intratumoral neutrophils is significantly correlated with the early recurrence which could be a poor prognostic factor¹⁴. In our *kras*^{V12}-expressing zebrafish liver tumor model, Infiltrations of TAMs and TANs are significantly higher in male tumors than in female tumors. Pro-tumor genes are also more strongly expressed in the TAMs and TANs of male tumors, correlating to a faster tumor progression¹⁵.

As we previously reported, the activation of stromal cells has a close correlation with tumor progression, especially HSCs, TAMs and TANs^{11, 15, 16}. Interestingly, these stromal cells appear to also contribute to the sex disparity of HCC in the *kras*^{V12} model. In male *kras*^{V12} transgenic zebrafish, a higher level of serotonin activates HSCs and causes accelerated liver tumor progression¹¹. Male *kras*^{V12} transgenic zebrafish also produced higher of cortisol to cause enhanced TAN and TAM infiltration to accelerate liver tumor progression¹⁵. However, whether the importance of these stromal cells is universal to other oncogene-induced tumors or only specific to *kras*^{V12}-induced tumors remains unclear. Previously, our laboratory has generated two other oncogene induced HCC models in transgenic zebrafish; one is by inducible expression of *xmrk* oncogene¹⁷ and the other is inducible expression of the mouse *Myc* oncogene¹⁸. Both transgenic lines have been generated with the same Tet-on transgenic system where the oncogenes are expressed under the hepatocyte-specific *fabp10a* promoter and the expression was induced only by addition of the chemical inducer, doxycycline. In the present study, we first confirmed the sex disparity in HCC development in these two oncogene transgenic models. Then we found that positive correlations of these stroma cells to the progression of liver tumors in both the *xmrk* and *Myc* transgenic models, including conserved molecular pathways such as serotonin activated HSCs and cortisol enhanced TANs and TAMs. These mechanisms also similarly contribute to sex disparity of liver tumors in the *xmrk* and *Myc* models.

Results

Enhanced cell proliferation during hepatocarcinogenesis in male zebrafish with transgenic expression of *xmrk* or *Myc* oncogene. As we reported previously, *kras*^{V12}-expressing male tumors shows an accelerated HCC progression^{11, 15, 19}. To investigate if *xmrk*- or *Myc*-induced HCC has similar sex disparity, male and female *xmrk*⁺ or *Myc*⁺ fish were exposed to doxycycline for 7 days. 2D liver size was measured after the treatment (Fig. 1A). In the *xmrk*⁺ and *Myc*⁺ expressing fish of both sexes, male tumor livers were bigger than the female tumor livers in both *xmrk* and *Myc*-expressing fish (Fig. 1B). Histologically, male developed more

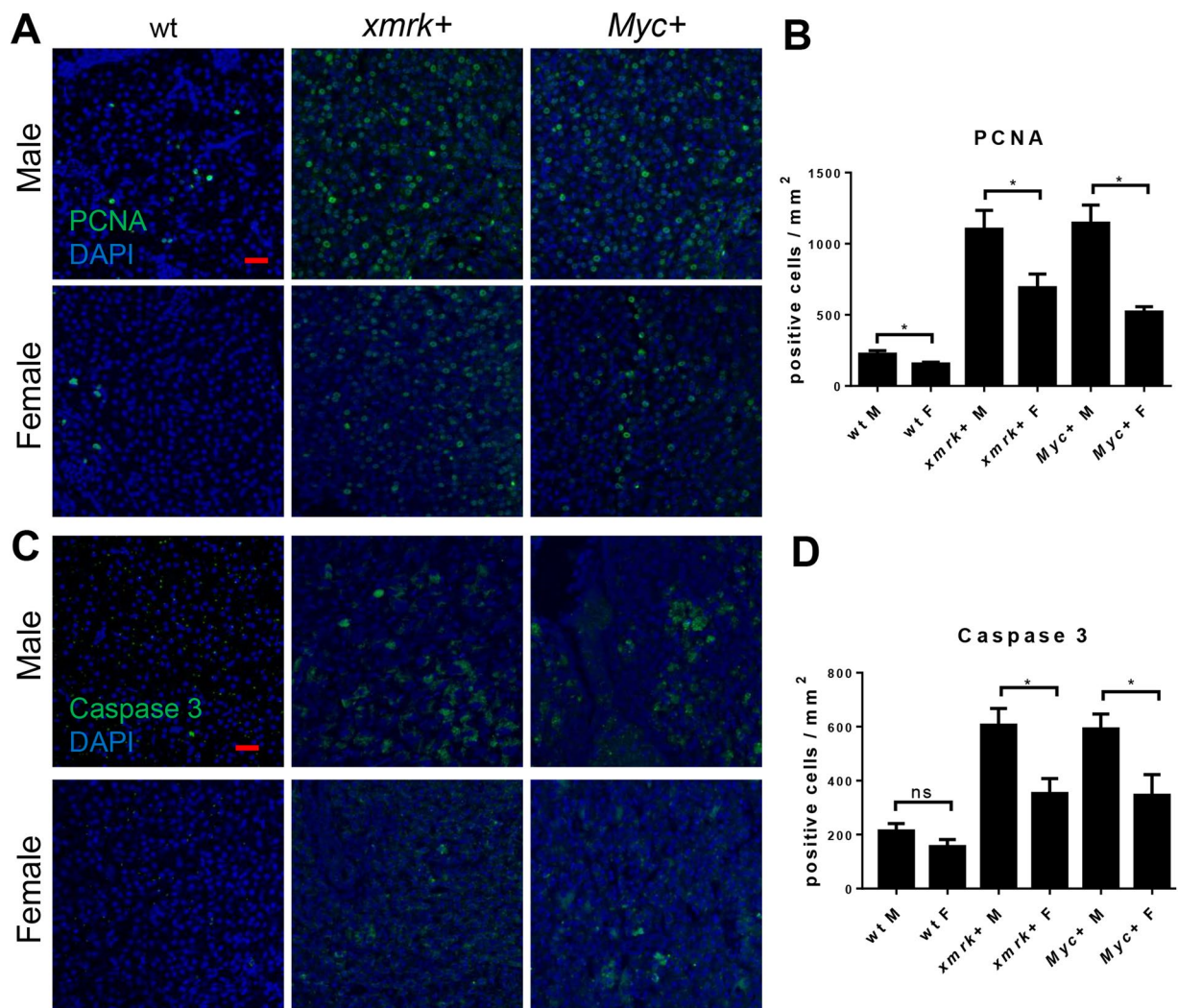


Figure 2. Proliferation and apoptosis in the livers of male and female *xmrk+* and *Myc+* fish following oncogene activation. 10 fish were analysed in each group and the experiment was repeated multiple times. Proliferation and apoptosis were examined by PCNA and Caspase 3 staining respectively. (A) IF staining of PCNA in liver sections. (B) Quantification of densities of proliferating liver cells (PCNA+). (C) IF staining of Caspase-3 in liver sections. (D) Quantification of densities of apoptotic liver cells (Caspase 3+). * $P < 0.05$. Scale bars: 20 μm .

aggressive tumors than female in *xmrk*-expressing liver. In wildtype livers, the 2-cell hepatic plate was well organized while in *xmrk*-expressing male tumor, oncogenic hepatocytes had prominent and multiple nucleoli and lost the 2-cell plate organization (Fig. 1C). In *xmrk*-expressing female tumors, most of the tumors were at early HCC stage with loss of 2-cell plate and prominent nucleoli. However, in *Myc*-expressing fish, all of the liver tumors were at the hyperplastic stage without apparent sex disparity. As summarized in Fig. 1D, 50% of male *xmrk*-expressing tumor showed carcinoma, 30% showed adenoma and the remaining 20% had hepatic hyperplasia. In contrast, 80% of female *xmrk*-expressing tumor showed hepatic hyperplasia and the remaining 20% had adenoma histology. However, the *Myc*-expressing livers in both female and male had similar hepatic hyperplasia histology.

To further investigate the molecular mechanism in both transgenic lines, the cell proliferation and apoptosis were examined by immunofluorescence (IF) staining of PCNA and caspase-3, respectively. The proliferating cells were comparable and had a low percentage in both sexes of normal livers of wildtype fish, while *xmrk* and *Myc*-expression promoted hepatocyte proliferation significantly (Fig. 2A,B). Levels of hepatocyte apoptosis had also been accelerated by *xmrk* and *Myc*-expression in both sexes (Fig. 2C,D). In wildtype fish, there were no significant difference in both proliferating cells and apoptotic cells between female and male.

Correlation of serotonin level, activated HSCs and higher induction of male carcinogenesis. Previously we have found that both the density of total HSCs and the percentages of activated HSCs are significantly higher in male *kras*^{V12}-induced liver tumors than female *kras*^{V12}-induced liver tumors¹¹. As a higher HSC density also indicates a poor prognosis in HCC patients²⁰, HSC density and activation ratio were determined in *xmrk* and *Myc*-expressing model. Glial fibrillary acidic protein (Gfap) has been used as a marker of

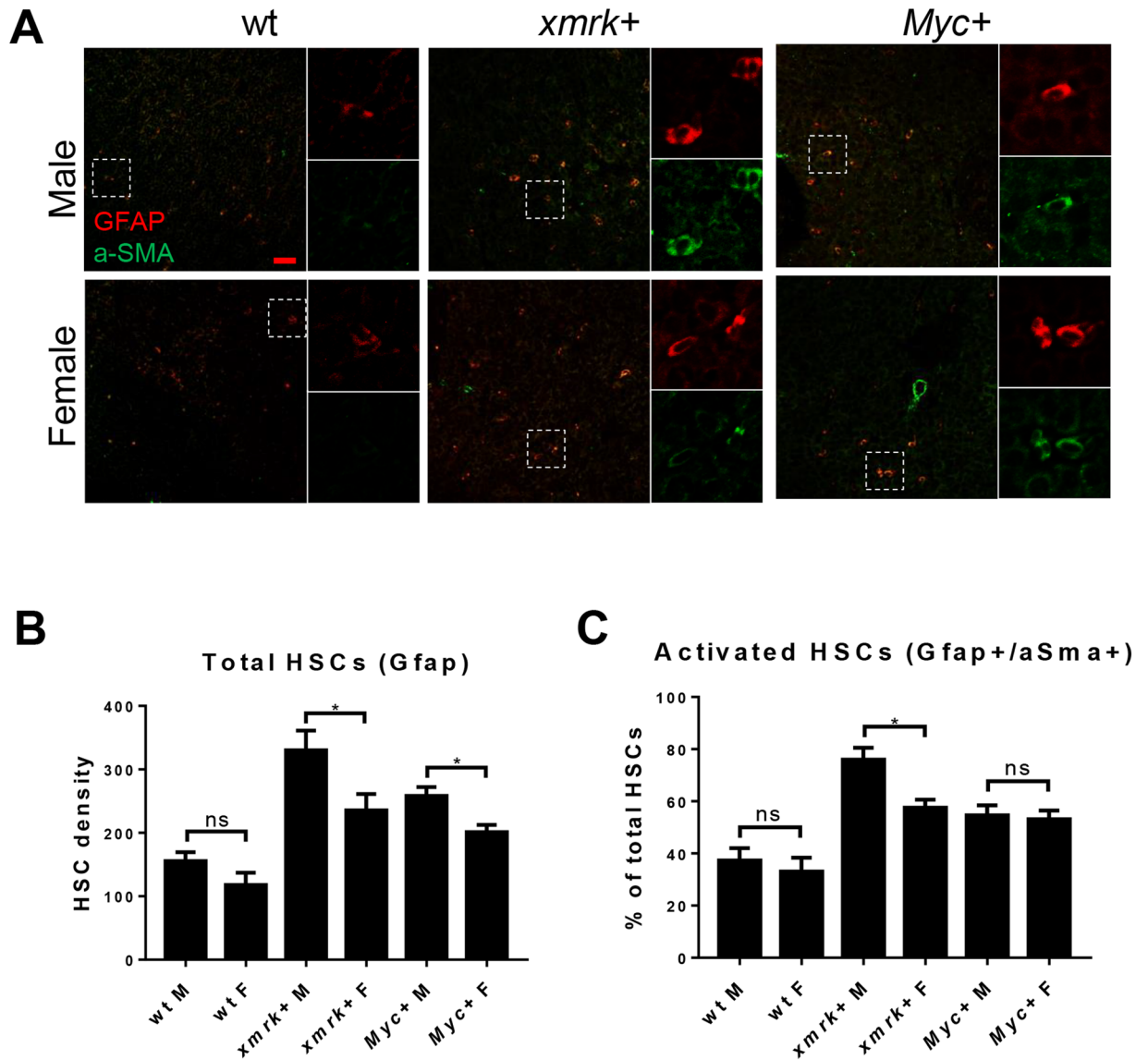


Figure 3. Determination of HSCs and activated HSCs in the livers of male and female *xmrk+* and *Myc+* fish following oncogene activation. 10 fish were analyzed in each group and the experiment was repeated once for reproducibility. (A) IF co-staining of GFAP (red) and a-SMA (green) in liver sections. White boxes indicate the enlarged area as shown on the right. (B) Quantification of total HSC density in liver sections. (C) Quantification of activated ratio of HSCs in liver sections. * $P < 0.05$. Scale bars: 20 μm .

HSCs as it marks both quiescent and activated HSC²¹. A-SMA (alpha smooth muscle Actin), in contrast, only labels the activated HSC²². By immunofluorescence (IF) co-staining of Gfap and a-SMA, both quiescent and activated HSC could be detected. As shown in Fig. 3A and B, Gfap marked total HSCs were increased in *xmrk*- and *Myc*-expressing livers with a higher density in males than in females. A-SMA+/Gfap+ cells indicated activated HSCs and the percentage of activated HSCs was also significantly increased after overexpression of *xmrk* or *Myc*, but the sex disparity only existed in the *xmrk*-expressing model (Fig. 3A,C).

Serotonin has been shown to specifically activate HSCs through 5-hydroxytryptamine receptor 2B (Htr2b)⁹ and there is a higher level of serotonin in the *kras*^{V12}-expressing livers in male zebrafish than female zebrafish¹¹. Tryptophan hydroxylase 1b (Tph1b) is the rate limiting enzyme of serotonin synthesis²³. To investigate if *xmrk* and *Myc*-expressing liver also have the sex difference in the serotonin level, IF staining of serotonin with HNF4 α (hepatocyte nuclear factor 4 alpha, for marking the hepatocytes) as well as IF staining of phos-Tph1 with HNF4 α were carried out. In both *xmrk*- and *Myc*-expressing livers, males had a higher level of serotonin than females (Fig. 4A,B). Compare between *xmrk*- and *Myc*-expressing livers in the same sex, *xmrk*-expressing liver tumors had a higher serotonin level than *Myc*-expressing liver tumor. IF staining of phos-Tph1 led to similar and consistent results. Phos-Tph1 was higher in males than in females in *xmrk* and *Myc*-expressing liver (Fig. 4C,D). Male fish had higher levels of phos-Tph1 than female fish across all three comparing groups and male *xmrk*-expressing tumor had a higher phos-Tph1 level than *Myc*-expressing tumor.

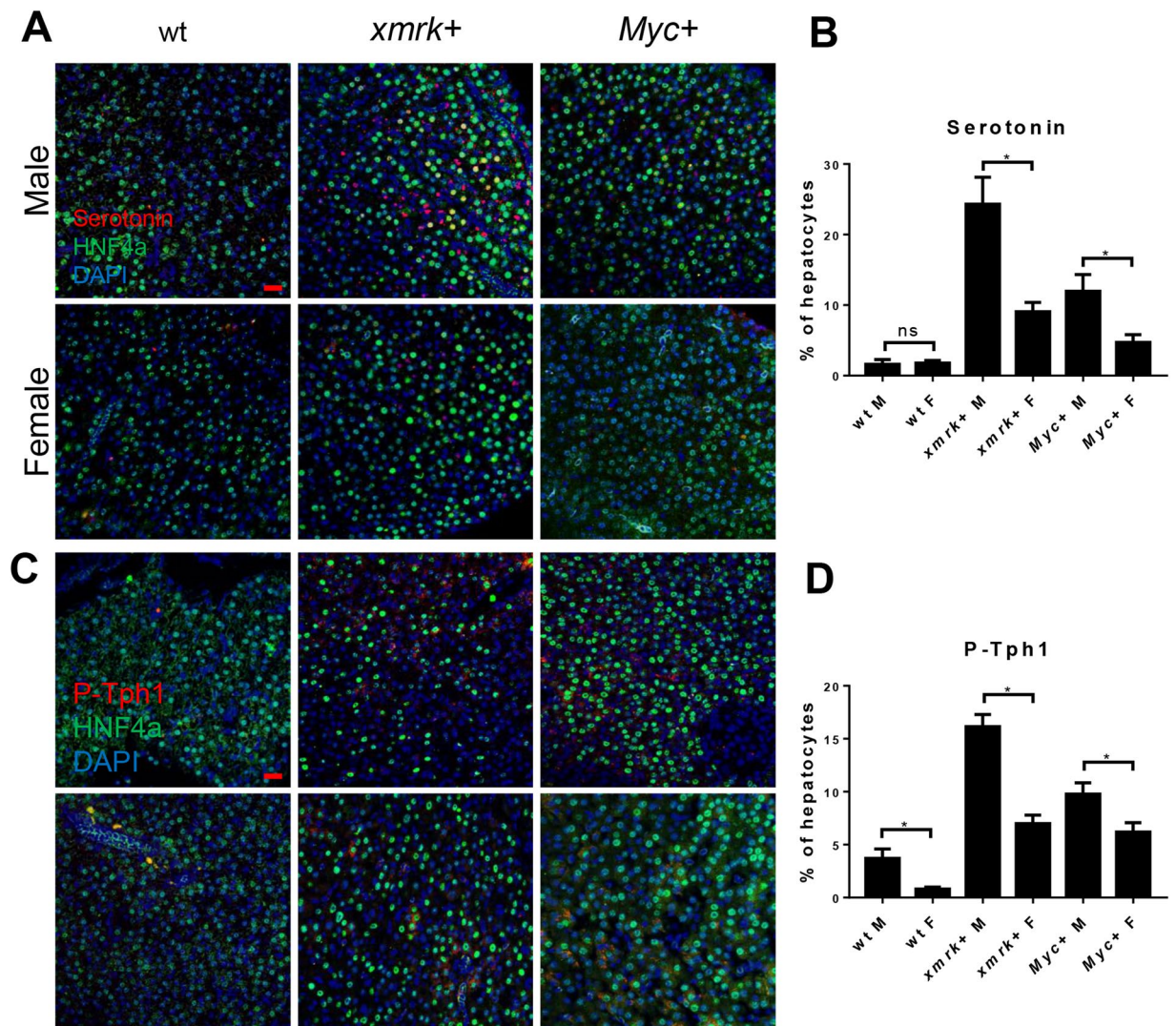


Figure 4. Immunofluorescent staining for serotonin and P-Tph1 in the livers of male and female *xmrk+* and *Myc+* fish following oncogene activation. 10 fish were analyzed in each group and the experiment was repeated once for reproducibility. (A) IF co-staining of serotonin (red) and HNF4a (green) in liver sections. (B) Quantification of ratio of serotonin-producing hepatocytes in liver sections. (C) IF co-staining of P-Tph1 (red) and HNF4a (green) in liver sections. (D) Quantification of ratio of P-Tph1-expressed hepatocytes in liver sections. * $P < 0.05$. Scale bars: 20 μm . ns, non-significance.

Correlation of cortisol level, TAMs/TANs and higher induction of male carcinogenesis. In HCC patients, immune cell density has a close correlation with tumor progression and could be a poor prognostic factor of HCC¹⁴. In our previously reported *kras*^{V12} expressing zebrafish model, TAN and TAM infiltrations were much severer in male fish than in female fish¹⁵. To investigate the immune cell infiltration in *xmrk*- and *Myc*-expressing livers, IF co-staining of Csf1r (colony stimulating factor 1 receptor) and Lcp (L. pneumophila-containing phagosome) were conducted. Csf1r is a macrophage-specific receptor which controls the differentiation and survival of macrophages²⁴. Lcp marks both neutrophils and macrophages²⁵. By co-staining of Csf1r and Lcp, neutrophils and macrophages could be identified simultaneously. In both *xmrk*- and *Myc*-expressing liver tumors, neutrophils and macrophages were significantly higher in males than in females (Fig. 5A,C). Compare between the same sex, *xmrk*- or *Myc*-expressing liver tumors had the similar density of neutrophils and macrophages.

Cortisol has been shown to affect neutrophil and macrophage gene expression profile^{26,27}. In *kras*^{V12}-expressing livers, cortisol is upregulated after *kras*^{V12} expression with a higher level of production in male liver tumors, which in turn induces Tgfb1a expression¹⁵. To investigate if similar phenomena existed in *xmrk*- and *myc*-expressing livers, levels of cortisol and Tgfb1a were examined by IF staining together with Hnf4 α . As shown in Fig. 6A,B, cortisol was only greatly upregulated in male *xmrk*-expressing livers. In both sexes of *Myc*-expressing livers, cortisol remained at the same level to that in wildtype fish. Tgfb1a expression was higher in both male *xmrk*- and *myc*-expressing livers than those in female counterparts (Fig. 6C,D). It has been well documented that Tgfb1a promotes tumor progression through polarization of TANs and TAMs²⁸. Here, the Tgfb1a expression showed a consistent sex disparity with TAN/TAM density and tumor progression in *xmrk*- and *Myc*-expressing tumors.

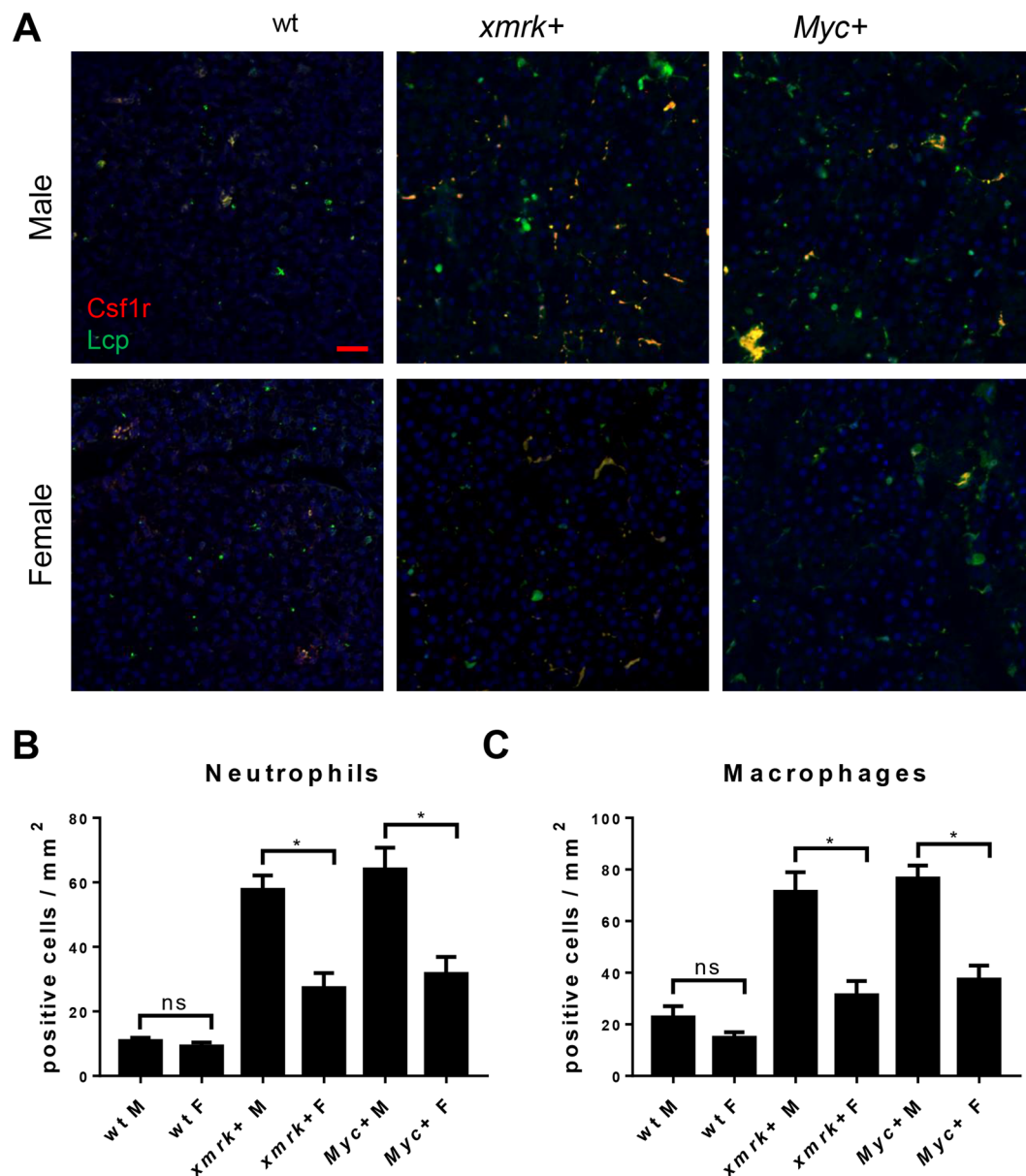


Figure 5. Determination of neutrophils and macrophages in the livers of male and female *xmrk+* and *Myc+* fish following oncogene activation. 10 fish were analyzed in each group and the experiment was repeated once for reproducibility. (A) IF co-staining of Csf1r (red) and Lcp (green) in liver sections. (B) Quantification of neutrophil densities in liver sections. (C) Quantification of macrophage densities in liver sections. * $P < 0.05$. Scale bars: 20 μm .

Discussion

In recent years, increasing evidence indicates that the crosstalk between the cancer cells and stromal cells plays a significant role in tumor progression²⁹. In human patients, MYC triggers hepatocyte proliferation and is associated with liver fibrosis. Myc overexpression in an HCC mice model activates HSCs and facilitates liver fibrosis³⁰. *Xmrk* is a fish oncogene and is basically a mutated form of EGFR with hyperactivity³¹. In human HCC patients, EGFR mutations also cause increased tumor infiltration of immune cells and necrosis³². Thus, both oncogenes studied in the present report are actively involved in stromal cell activities in human tumors.

In our previous studies on *kras*^{V12}-expressing liver tumors in the zebrafish, stromal cells including HSCs, neutrophils and macrophages are activated after *kras*^{V12} oncogene induction. We have observed that following induction of *kras*^{V12} expression, both total HSCs and activated HSCs are increased and so is infiltration of neutrophils and macrophages in the *kras*^{V12}-expressing liver tumors¹⁵. In the present study, consistent observations were also made in the *xmrk*- and *Myc*-expressing liver tumors. In the previous studies, we have also found that serotonin level is crucial for HSC activation¹¹; this is consistent in the *xmrk*- and *Myc*-expressing liver tumors. Recently, the involvement of serotonin in human HCC and identification of plasma serotonin as a marker for HCC diagnosis have been reported³³. Our studies in the zebrafish liver tumor models should help elucidate

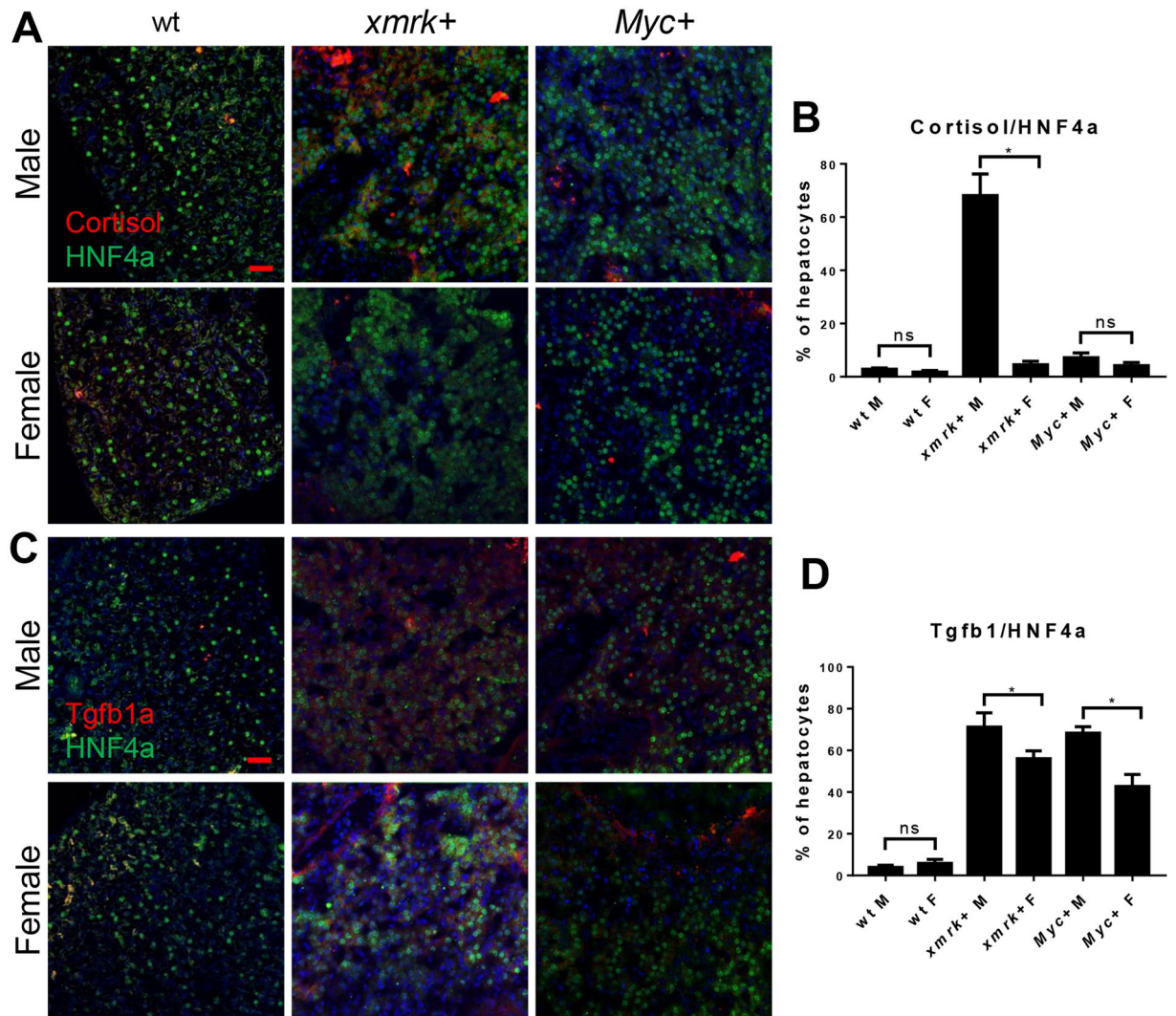


Figure 6. Immunofluorescent staining for cortisol and Tgfb1a in the livers of male and female *xmrk+* and *Myc+* fish following oncogene activation. 10 fish were analyzed in each group and the experiment was repeated once for reproducibility. (A) IF co-staining of cortisol (red) and HNF4a (green) in liver sections. (B) Quantification of ratio of cortisol-expressing hepatocytes in liver sections. (C) IF co-staining of Tgfb1a (red) and HNF4a (green) in liver sections. (D) Quantification of ratio of Tgfb1a-expressing hepatocytes in liver sections.

the potential mechanism of how serotonin promote HCC progression. As the importance of serotonin in HCC has been observed consistently in three different oncogene-induced liver tumors in the zebrafish models, the serotonin-mediated mechanism in HCC could be quite universal and thus our zebrafish studies support the use of serotonin as a promising diagnostic marker of HCC.

In the *kras*^{V12}-expressing liver tumor model in zebrafish, there is an apparent sex disparity with significantly faster liver tumor progression in males than in females^{11, 15, 19}. In the present study, we found the same sex disparity on HCC progression in the *xmrk* model and, to a less extent, in the *Myc* model. One week of oncogene activation causes apparent HCC in some of the male fish of both *kras*- and *xmrk*-expressing tumors, while the female *kras*- and *xmrk*-expressing fish could only reach the adenoma stage. In contrast, both male and female *Myc*-expressing fish were only at the hyperplastic stage without much discrimination histologically; however, molecularly, male *Myc* fish had more proliferating and apoptotic cells than female *Myc* fish (Fig. 2). These observations are consistent with our initial reports of these oncogene transgenic models over a longer term (a few months) of oncogene activation, in which *kras+* and *xmrk+* fish could develop advanced HCC while *Myc+* fish generally develop only adenoma^{17, 18, 34}.

Previous studies in the *kras*^{V12}-induced liver tumor models in zebrafish have also shown that the higher level of cortisol induced stronger Tgfb1a expression in male *kras*^{V12}-expressing tumors to attract more neutrophils and macrophages, thus stimulating tumor progression¹⁵. In *xmrk* and *Myc*-expressing tumor, we found that intra-tumoral TAN and TAM density were higher in male liver tumors than in female liver tumors. However, the increased cortisol in the liver was observed only in male *xmrk+* fish but not significantly in male *Myc+* fish.

Nevertheless, TAN and TAM infiltrations were similarly higher in males than in females in both *xmrk*⁺ and *Myc*⁺ fish, which may indicate that other signals maybe responsible for sex-biased activation of TANs and TAMs in *Myc*-induced liver tumors.

Compared to our previous findings in the *kras* model^{11, 15}, we found that the *xmrk* overexpression model showed more similar characteristics to the *kras* model in activation of stromal cells including HSCs, neutrophils and macrophages during liver tumor initiation. This is also consistent with our previous observation by transcriptomic analysis that the *xmrk* and *kras* liver tumors models have more similar deregulated pathways compared to that in the *Myc* liver tumor model³⁵. In the present study, we also found that the *Myc* model has a mild sex disparity in liver tumorigenesis and this may be due to a slower progression of the liver tumor in the *Myc* model; for example, histologically diagnosed HCC could be induced in the *kras* and *xmrk* models within one week of oncogene activation while it may takes 4 months to develop HCC under a high dose of induction in the *Myc* model^{17, 18, 34}. Similarly in mouse, *Myc* overexpression could only lead to less severe liver tumors instead of development of HCC *in vivo*³⁶.

HCC develops from chronic inflammatory and/or fibrosis tissue, which promote tumor progression and resist medical therapy. A better understanding of the interaction between tumor cells and various stromal cells as well as relevant signaling pathways should help gain more knowledge on potential mechanisms in tumor progression. A better understanding of sex disparity of liver cancer should be important for identification of sex-based therapeutic targets and thus for improving therapeutic efficiency.

Methods

Zebrafish Husbandry. All zebrafish experiments were carried out in accordance with the recommendations in the Guide for the Care and Use of Laboratory Animals of the National Institutes of Health and the protocol was approved by the Institutional Animal Care and Use Committee (IACUC) of the National University of Singapore (Protocol Number: 096/12), *Tg(fabp10:TA; TRE:xmrk; krt4:GFP)*¹⁷ and *Tg(fabp10:TA; TRE:Myc; krt4:GFP)*¹⁸ zebrafish in a Tet-on system for inducible hepatocyte-specific expression of oncogenic *xmrk* and *Myc* were used in this study and referred to as *xmrk* and *Myc*, respectively.

Induction of transgene expression and gross examination. Induction of transgene expression were conducted in 3-month-old adult fish for 7 days with 60 µg/ml doxycycline (D9891; Sigma). In preliminary experiments, we found no histological change of liver histology after one day of doxycycline induction but histological transformation of liver cells (hyperplasia) was observed from 3 days post-induction (data not shown). At the end of doxycycline treatment, >10 fish in each group were used for imaging analyses. All the zebrafish were anesthetized in 0.08% tricaine (E10521; Sigma) and immobilized in 3% methylcellulose (M0521; Sigma) before imaging. Each fish was photographed individually from the left lateral side with an Olympus microscope.

Histological and immunocytological Analyses. All of the adult livers were fixed in 4% paraformaldehyde in phosphate-buffered saline (P6748; Sigma) overnight, embedded in paraffin, and sectioned at 5-mm thickness using a microtome, followed by hematoxylin and eosin (H&E), immunohistochemistry (IHC), or immunofluorescence (IF) stainings. H&E (H-3404; Vector) staining were conducted according to the manufacturers' protocols. For IHC and IF-stainings, the primary antibodies derived from rabbit or mouse were purchased commercially, including anti-PCNA (FL-261; Santa Cruz Biotechnology, Dallas, TX), anti-caspase 3 (C92-065; BD Biosciences, Singapore), anti-Gfap (154474; Abcam, Singapore), anti- α -smooth muscle actin (a-Sma) (ab15734; Abcam, Singapore), anti-serotonin (C5545; Sigma, USA), anti-PTph (SC135716; Santa Cruz, CA, USA), anti-Hnf4a (MA5-14891; Thermo, Singapore), anti-Lcp (40898; GeneTex, USA), anti-Csf1r (128677; GeneTex, USA), anti-cortisol (C8409; Sigma, USA) and anti-Tgfb1a (55450; Anaspec, CA, USA). Anti-rabbit or anti-mouse secondary antibodies were purchased from Thermo Fisher Scientific (Singapore). At least eight fish from each treatment group were examined and one high-power field was selected randomly from each fish liver as a representative image. IF signals were counted manually for quantitative analyses.

Statistical Analysis. For statistical significance between two groups, 2-tailed unpaired Student *t* test was performed using GraphPad Prism version 7.00 for Windows. Statistical data are presented as means \pm SEM. Same statistical results were obtained by one way ANOVA analysis.

References

- Lee, C. M. *et al.* Age, gender, and local geographic variations of viral etiology of hepatocellular carcinoma in a hyperendemic area for hepatitis B virus infection. *Cancer* **86**, 1143–1150 (1999).
- Yeh, S. H. & Chen, P. J. Gender disparity of hepatocellular carcinoma: the roles of sex hormones. *Oncology* **78**(Suppl 1), 172–179, doi:10.1159/000315247 (2010).
- Nakatani, T., Roy, G., Fujimoto, N., Asahara, T. & Ito, A. Sex hormone dependency of diethylnitrosamine-induced liver tumors in mice and chemoprevention by leuprorelin. *Jpn J Cancer Res* **92**, 249–256 (2001).
- Di Maio, M. *et al.* Hormonal treatment of human hepatocellular carcinoma. *Ann N Y Acad Sci* **1089**, 252–261, doi:10.1196/annals.1386.007 (2006).
- Yeh, Y. T., Chang, C. W., Wei, R. J. & Wang, S. N. Progesterone and related compounds in hepatocellular carcinoma: basic and clinical aspects. *BioMed research international* **2013**, 290575, doi:10.1155/2013/290575 (2013).
- Chow, P. K. *et al.* Randomised double-blind trial of megestrol acetate vs placebo in treatment-naive advanced hepatocellular carcinoma. *British journal of cancer* **105**, 945–952, doi:10.1038/bjc.2011.333 (2011).
- Chow, P. K. *et al.* High-dose tamoxifen in the treatment of inoperable hepatocellular carcinoma: A multicenter randomized controlled trial. *Hepatology* **36**, 1221–1226, doi:10.1053/jhep.2002.36824 (2002).
- Coulouarn, C. *et al.* Hepatocyte-stellate cell cross-talk in the liver engenders a permissive inflammatory microenvironment that drives progression in hepatocellular carcinoma. *Cancer Res* **72**, 2533–2542, doi:10.1158/0008-5472.CAN-11-3317 (2012).
- Ebrahimkhani, M. R. *et al.* Stimulating healthy tissue regeneration by targeting the 5-HT(2)B receptor in chronic liver disease. *Nat Med* **17**, 1668–1673, doi:10.1038/nm.2490 (2011).

10. Sun, B. *et al.* Intratumoral hepatic stellate cells as a poor prognostic marker and a new treatment target for hepatocellular carcinoma. *PLoS One* **8**, e80212, doi:10.1371/journal.pone.0080212 (2013).
11. Yang, Q., Yan, C., Yin, C. & Gong, Z. Serotonin Activated Hepatic Stellate Cells Contribute to Sex Disparity in Hepatocellular Carcinoma. *Cell Mol Gastroenterol Hepatol* **3**, 484–499, doi:10.1016/j.jcmgh.2017.01.002 (2017).
12. Allavena, P., Sica, A., Solinas, G., Porta, C. & Mantovani, A. The inflammatory micro-environment in tumor progression: the role of tumor-associated macrophages. *Crit Rev Oncol Hematol* **66**, 1–9, doi:10.1016/j.critrevonc.2007.07.004 (2008).
13. Naugler, W. E. *et al.* Gender disparity in liver cancer due to sex differences in MyD88-dependent IL-6 production. *Science* **317**, 121–124, doi:10.1126/science.1140485 (2007).
14. Li, Y. W. *et al.* Intratumoral neutrophils: a poor prognostic factor for hepatocellular carcinoma following resection. *J Hepatol* **54**, 497–505, doi:10.1016/j.jhep.2010.07.044 (2011).
15. Yan, C., Yang, Q. & Gong, Z. Tumor-Associated Neutrophils and Macrophages Promote Gender Disparity in Hepatocellular Carcinoma in Zebrafish. *Cancer Res* **77**, 1395–1407, doi:10.1158/0008-5472.CAN-16-2200 (2017).
16. Yan, C., Huo, X., Wang, S., Feng, Y. & Gong, Z. Stimulation of hepatocarcinogenesis by neutrophils upon induction of oncogenic kras expression in transgenic zebrafish. *J Hepatol* **63**, 420–428, doi:10.1016/j.jhep.2015.03.024 (2015).
17. Li, Z. *et al.* Inducible and repressible oncogene-addicted hepatocellular carcinoma in Tet-on xmrk transgenic zebrafish. *J Hepatol* **56**, 419–425, doi:10.1016/j.jhep.2011.07.025 (2012).
18. Li, Z. *et al.* A transgenic zebrafish liver tumor model with inducible Myc expression reveals conserved Myc signatures with mammalian liver tumors. *Disease models & mechanisms* **6**, 414–423, doi:10.1242/dmm.010462 (2013).
19. Li, Y., Li, H., Spitsbergen, J. M. & Gong, Z. Males develop faster and more severe hepatocellular carcinoma than females in krasV12 transgenic zebrafish. *Sci Rep* **7**, 41280, doi:10.1038/srep41280 (2017).
20. Ji, J. *et al.* Hepatic stellate cell and monocyte interaction contributes to poor prognosis in hepatocellular carcinoma. *Hepatology* **62**, 481–495, doi:10.1002/hep.27822 (2015).
21. Morini, S. *et al.* GFAP expression in the liver as an early marker of stellate cells activation. *Ital J Anat Embryol* **110**, 193–207 (2005).
22. Carpino, G. *et al.* Alpha-SMA expression in hepatic stellate cells and quantitative analysis of hepatic fibrosis in cirrhosis and in recurrent chronic hepatitis after liver transplantation. *Dig Liver Dis* **37**, 349–356, doi:10.1016/j.dld.2004.11.009 (2005).
23. Fitzpatrick, P. F. Tetrahydropterin-dependent amino acid hydroxylases. *Annu Rev Biochem* **68**, 355–381, doi:10.1146/annurev.biochem.68.1.355 (1999).
24. Pyonteck, S. M. *et al.* CSF-1R inhibition alters macrophage polarization and blocks glioma progression. *Nat Med* **19**, 1264–1272, doi:10.1038/nm.3337 (2013).
25. Meijer, A. H. *et al.* Identification and real-time imaging of a myc-expressing neutrophil population involved in inflammation and mycobacterial granuloma formation in zebrafish. *Dev Comp Immunol* **32**, 36–49, doi:10.1016/j.dci.2007.04.003 (2008).
26. Castro, R., Zou, J., Secombes, C. J. & Martin, S. A. Cortisol modulates the induction of inflammatory gene expression in a rainbow trout macrophage cell line. *Fish Shellfish Immunol* **30**, 215–223, doi:10.1016/j.fsi.2010.10.010 (2011).
27. Davis, J. M. *et al.* Increased neutrophil mobilization and decreased chemotaxis during cortisol and epinephrine infusions. *J Trauma* **31**, 725–731; discussion 731–722 (1991).
28. Fridlender, Z. G. *et al.* Polarization of tumor-associated neutrophil phenotype by TGF-beta: “N1” versus “N2” TAN. *Cancer Cell* **16**, 183–194, doi:10.1016/j.ccr.2009.06.017 (2009).
29. Bremnes, R. M. *et al.* The role of tumor stroma in cancer progression and prognosis: emphasis on carcinoma-associated fibroblasts and non-small cell lung cancer. *J Thorac Oncol* **6**, 209–217, doi:10.1097/JTO.0b013e3181f8a1bd (2011).
30. Nevzorova, Y. A. *et al.* Overexpression of c-myc in hepatocytes promotes activation of hepatic stellate cells and facilitates the onset of liver fibrosis. *Biochim Biophys Acta* **1832**, 1765–1775, doi:10.1016/j.bbadis.2013.06.001 (2013).
31. Gomez, A., Wellbrock, C., Gutbrod, H., Dimitrijevic, N. & Scharlt, M. Ligand-independent dimerization and activation of the oncogenic Xmrk receptor by two mutations in the extracellular domain. *J Biol Chem* **276**, 3333–3340, doi:10.1074/jbc.M006574200 (2001).
32. Brzezniak, C. *et al.* RRX-001-Induced Tumor Necrosis and Immune Cell Infiltration in an EGFR Mutation-Positive NSCLC with Resistance to EGFR Tyrosine Kinase Inhibitors: A Case Report. *Case Rep Oncol* **9**, 45–50, doi:10.1159/000443605 (2016).
33. Abdel-Razik, A. *et al.* Could serotonin be a potential marker for hepatocellular carcinoma? A prospective single-center observational study. *Eur J Gastroenterol Hepatol* **28**, 599–605, doi:10.1097/MEG.0000000000000569 (2016).
34. Chew, T. W. *et al.* Crosstalk of Ras and Rho: activation of RhoA abates Kras-induced liver tumorigenesis in transgenic zebrafish models. *Oncogene* **33**, 2717–2727, doi:10.1038/onc.2013.240 (2014).
35. Zheng, W. *et al.* Xmrk, kras and myc transgenic zebrafish liver cancer models share molecular signatures with subsets of human hepatocellular carcinoma. *PLoS One* **9**, e91179, doi:10.1371/journal.pone.0091179 (2014).
36. Zender, L. *et al.* Generation and analysis of genetically defined liver carcinomas derived from bipotential liver progenitors. *Cold Spring Harb Symp Quant Biol* **70**, 251–261, doi:10.1101/sqb.2005.70.059 (2005).

Acknowledgements

This work was supported by grants from Ministry of Education of Singapore (R154000667112 and R154000A23112).

Author Contributions

Q.Y., C.Y. and Z.G. conceived the experiments and wrote the paper. Q.Y. and C.Y. performed the experiments and analyzed data.

Additional Information

Competing Interests: The authors declare that they have no competing interests.

Publisher's note: Springer Nature remains neutral with regard to jurisdictional claims in published maps and institutional affiliations.



Open Access This article is licensed under a Creative Commons Attribution 4.0 International License, which permits use, sharing, adaptation, distribution and reproduction in any medium or format, as long as you give appropriate credit to the original author(s) and the source, provide a link to the Creative Commons license, and indicate if changes were made. The images or other third party material in this article are included in the article's Creative Commons license, unless indicated otherwise in a credit line to the material. If material is not included in the article's Creative Commons license and your intended use is not permitted by statutory regulation or exceeds the permitted use, you will need to obtain permission directly from the copyright holder. To view a copy of this license, visit <http://creativecommons.org/licenses/by/4.0/>.

© The Author(s) 2017